

SNR Penalty from the Path-loss Disparity in Virtual Multiple-Input-Single-Output (VMISO) Link

Haejoon Jung and Mary Ann Ingram

School of Electrical and Computer Engineering, Georgia Institute of Technology, Atlanta, GA 30332-0250, USA

Email: {hjung35, mai}@gatech.edu

Abstract—Cooperative transmission (CT), in which spatially separated wireless nodes collaborate to form a virtual antenna array or virtual multiple-input-multiple-output (VMISO) link, is an effective technique to mitigate multi-path fading by spatial diversity. In this paper, we study the disparities in path losses between the randomly placed relay nodes in a transmit cluster and the destination nodes. Many authors assume that the elements in a virtual antenna array are co-located, even though they are spread out. In this paper, we show that a signal-to-noise-ratio (SNR) penalty of up to 3dB should be included when making this assumption. By the high-SNR approximation of the outage rates, we show that the performance degradation caused by the path-loss disparity can be characterized equivalently by log-normal shadowing. Moreover, we derive the upper and lower bounds of the real outage probabilities in closed forms based on the log-normal shadowing model, by which we can estimate the SNR penalty of the co-located assumption.

I. INTRODUCTION

For small wireless nodes with limited power, where collocated antennas (a real antenna array) cannot be deployed, cooperative transmission (CT) is an alternative way to achieve spatial diversity in fading channel [1], [2]. CT provides an SNR advantage through array and diversity gains by creating a virtual multiple-input-single-output (VMISO) link that connects a transmitting cluster (multiple nodes) with a single receiver node. Based on the SNR advantage of CT, various higher layer protocols have been proposed, in which the VMISO links provide gains at higher layers such as throughput improvement, energy saving, energy balancing, and range extension [3]–[6].

In such protocols, two abstraction models of the VMISO link are widely used to deal with random topologies in the network-scale analysis and simulations. First, when the node degree is high enough, the *continuum approximation* in [7] and [6] is used, in which the number nodes goes to infinity while the transmit power of each node becomes extremely small. However, this continuum model cannot be applied to the low node degree situation. The other abstraction model, intended for the low node degree case, assumes physically separated cooperating nodes in a cluster are simplified to be a single node with a multiple-antenna array as in [3]–[5]. In this *co-located approximation* model, the disparate path losses caused by the different distances between the transmitting nodes in a cluster to the receiver node are ignored. The authors in [8] realized through simulation of some specific topologies that

there can be a significant error (i.e., SNR penalty) incurred for making the co-located assumption.

Beaulieu et al. [2] derived a closed-form expression for the outage probability at the destination for the case of the decode-and-forward (DF) relays, where the location of the relays are assumed known. [2] has an intermediate result, where the number of relays that successfully decode is assumed known, while the final result in [2] allows for the opportunistic case, where the number of relays that successfully decode is not known a priori. However, this final expression in [2] is long, complicated, and numerically sensitive [1]. Moreover, the SNR penalty for the co-located assumption is not considered in [2], nor are random locations of nodes taken into account.

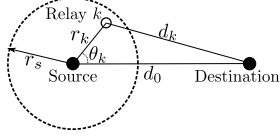
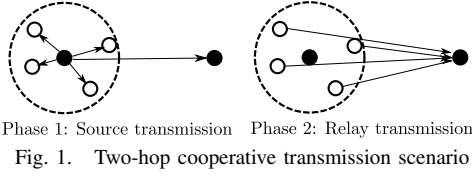
In this paper, we allow the node locations to be random. For the known number of successfully decoding relays, we show that the random locations of nodes produces a random received power, averaged over multi-path fading, with a log-normal distribution, as in shadowing. We also derive a lower bound based on assuming error-free source-relay links. We also treat the opportunistic case and derive an upper bound for the case when the number of relays that successfully decode is not known a priori by assuming the first-hop errors are independent and identically distributed (i.i.d.). These bounds provide the best and worst case SNR penalties for the co-located assumption. To our knowledge, this is the first study that models the SNR loss due to the random path-loss disparities in the VMISO links.

II. SYSTEM MODEL

We consider a VMISO communication consisting of two phases as shown in Fig. 1, where the source, which is indicated by the left black dot at the center of the dotted lined circle, first transmits a packet to the destination (the right black dot) in Phase 1. After that, the multiple relays (the white-filled circles) around the source decode and then forward (DF) using orthogonal channels to the destination in Phase 2 [2]. This cluster architecture is referred to as the centralized cluster [9], where each cluster has a cluster head that recruits its cooperating relays and triggers the group transmission.

A. Network Topology

We consider a static VMISO network as shown in Fig. 2, where the source node is located at the origin with a distance d_0 to the destination. Also, there are N number of cooperating



relays around the source, which are located in the dotted-lined circle with a radius r_s centered at the source node. r_s can be regarded as the SISO range, over which the source collects its cooperators. As in [3]–[5], we assume the “CT range extension case”, where $1.5 \leq d_0/r_s \leq 4$, which was demonstrated in [10]. We note that maximum range extension happens when radios do not decrease their transmit powers when cooperating, and when they transmit using either orthogonal channels or space-time-block-coding, so the link benefits from diversity gain [1]. The co-located VMISO model in [3]–[5] assumes that the links between the source and the relays are error-free, which is another factor that causes the error of the co-located approximation.

We assume that N relays are independently and identically distributed in the circle with the radius r_s following the uniform distribution. As shown in Fig. 2, Relay k represented by the white-filled circle exists at a distance of r_k from the source with an angle θ_k with respect to the line connecting the source and destination. Also, Relay k is d_k away from the destination, which determines the path loss between the relay and the destination. It follows that the polar coordinates (r_k, θ_k) of Relay k have the probability distribution functions (PDFs) of $f_{r_k}(r_k) = \frac{2r_k}{r_s^2}$ and $f_{\theta_k}(\theta_k) = \frac{1}{2\pi}$, where $0 < r_k \leq r_s$ and $0 \leq \theta_k \leq 2\pi$, respectively.

B. Channel Model

We assume mutually independent Rayleigh fading for any links between two nodes (the source, relays, and destination). The node indices of the source and destination are zero and $N + 1$. The complex channel gains are denoted by $h_{0:k}$ (from the source to Relay k), $h_{0:N+1}$ (from the source to the destination), and $h_{k:N+1}$ (from Relay k to the destination) with the relay node index $1 \leq k \leq N$. Hence, $\Omega_{i:j} = |h_{i:j}|^2$ follows the exponential distribution with a parameter $\lambda_{i:j}$ that is determined by the locations of Nodes i and j . Therefore, when the node locations are given, the cumulative distribution function (CDF) of Ω_k given $\lambda_{i:j}$ is expressed as $F_{\Omega_{i:j}|\lambda_{i:j}}(x) = 1 - e^{-\lambda_{i:j}x}$, where the conditional mean and variance are $\mathbb{E}\{\Omega_{i:j}|\lambda_{i:j}\} = 1/\lambda_{i:j}$ and $\text{VAR}\{\Omega_{i:j}|\lambda_{i:j}\} = 1/\lambda_{i:j}^2$, respectively. If the path loss exponent is α , then $\lambda_{0:k} = r_k^\alpha$ for the source-relay link and $\lambda_{k:N+1} = d_k^\alpha$ for the relay-destination link.

C. Outage Model

In this section, we first consider the outage probability for a deterministic network topology (i.e., the relay locations are given), the closed form of which is provided in [2]. However, while [1], [2] and other existing physical layer studies in CT assume a specific network topology, which is not random, we consider the random spatial distribution of the relays to capture the effect of the path-loss disparity.

Assuming the same transmission powers for the source and N relays, the conditional mutual information between the source and Relay k given that $\lambda_{0:k} = r_k^\alpha$ is $\mathbf{I}_{0:k}(\text{SNR}|\lambda_{0:k}) = \frac{1}{N+1} \log_2(1 + \text{SNR} \cdot \Omega_{0:k})$, where SNR is the transmit SNR of each node [2]. Therefore, for a certain transmission rate R (bit/Hz/sec), the probability that Relay k fails to decode the received signal from the source is given by

$$p_k = F_{\Omega_{0:k}|\lambda_{0:k}}(g(\text{SNR}, R)) = 1 - e^{-\lambda_{0:k} \cdot g(\text{SNR}, R)}, \quad (1)$$

where $F_{\Omega_{0:k}|\lambda_{0:k}}(x)$ is the conditional CDF of $\Omega_{0:k}$ given $\lambda_{0:k} = r_k^\alpha$, and $g(t, R) = (2^{(N+1)R} - 1)/t$.

Suppose that for a given network topology, \mathcal{S} is a particular set of M relays that successfully decode the source transmission, where $0 \leq M \leq N$. Therefore, the conditional mutual information of the VMISO link, conditioned on \mathcal{S} , is given by $\mathbf{I}(\text{SNR}|\mathcal{S}) = \frac{1}{N+1} \log_2(1 + \text{SNR} \cdot \Omega_{0:N+1} + \sum_{k \in \mathcal{S}} \text{SNR} \cdot \Omega_{k:N+1})$. Thus, the outage probability of the VMISO communication for a given network topology indicated by two parameter vectors $\bar{\Lambda}_s = [\lambda_{0:1}, \lambda_{0:2}, \dots, \lambda_{0:N}]^T$ and $\bar{\Lambda}_d = [\lambda_{1:N+1}, \lambda_{2:N+1}, \dots, \lambda_{N:N+1}]^T$ that satisfy $\lambda_{0:k} = r_k^\alpha$ and $\lambda_{k:N+1} = d_k^\alpha$ with $1 \leq k \leq N$ is expressed as $P_{out|\bar{\Lambda}_s, \bar{\Lambda}_d} = \sum_{\mathcal{S}} \Pr\{\mathbf{I} < R|\mathcal{S}\} \cdot \Pr\{\mathcal{S}\}$, where $\Pr\{\mathcal{S}\} = (\prod_{k \notin \mathcal{S}} p_k) \cdot (\prod_{k \in \mathcal{S}} (1 - p_k))$. This equation is the same as in [2] except that we suppose $\Pr\{\mathcal{S}\}$ is the probability conditioned on the certain network topology (i.e., $\bar{\Lambda}_s$ and $\bar{\Lambda}_d$). Considering the randomness of the relay locations, the outage rate averaged over the random network topology has N^2 -fold integral as

$$P_{out} = \int \dots \int P_{out|\bar{\Lambda}_s, \bar{\Lambda}_d} \times \prod_{k=1}^N [f_{\lambda_{0:k}, \lambda_{k:N+1}}(\lambda_{0:k}, \lambda_{k:N+1}) d\lambda_{0:k} d\lambda_{k:N+1}], \quad (2)$$

where $f_{\lambda_{0:k}, \lambda_{k:N+1}}(x_1, x_2)$ is the joint PDF of $\lambda_{0:k}$ and $\lambda_{k:N+1}$, which can be obtained by the variable transformation from $f_{r_k}(r_k)$ and $f_{\theta_k}(\theta_k)$.

III. OUTAGE RATE APPROXIMATION

A. First-hop Error Approximation

It is hard to obtain the closed form expression of the outage probability under the random relay locations in (2), because the first-hop (between the source and the relays) and second-hop (between the relays to the destination) depend on each other by the random relay locations. Therefore, to focus on the impact of the path-loss disparity in the second-hop, we approximate the first-hop error rates of the N relays by independent Bernoulli trials. The first-hop outage rate of Relay k in (1) satisfies that $0 \leq p_k \leq p_{max} = 1 - e^{-r_s^\alpha \cdot g(\text{SNR}, R)}$,

because $0 < r_k \leq r_s$. If all N relays have the same constant first-hop error rate of p , where $0 \leq p \leq p_{max}$, $P_{out|\bar{\Lambda}_s, \bar{\Lambda}_d}$ in Section II-C, which does not depend on $\bar{\Lambda}_s$ anymore, is simplified as

$$P_{out|\bar{\Lambda}_d} = \sum_{M=0}^N \binom{N}{M} p^{N-M} (1-p)^M \Pr \left[\sum_{k=0}^M \Omega_{k:N+1} < g(\text{SNR}, R) \right]. \quad (3)$$

In Section IV, the upper and lower bounds of outage capacity will be derived using $p = p_{max}$ and $p = 0$, respectively. If $Y = \sum_{k=0}^M \Omega_{k:N+1}$, then $\Pr \left[\sum_{k=0}^M \Omega_{k:N+1} < g(\text{SNR}, R) \right] = F_{Y|M, \bar{\Lambda}_d(1:M)}(g(\text{SNR}, R))$ that is the conditional CDF of Y for given M and a truncated vector with M elements out of N , $\bar{\Lambda}_d(1:M) = [\lambda_{1:N+1}, \dots, \lambda_{M:N+1}]^T$. Therefore, the final outage in (2) is approximated with N -fold integral by

$$\tilde{P}_{out} = \sum_{M=0}^N \binom{N}{M} p^{N-M} (1-p)^M \int \dots \int F_{Y|M, \bar{\Lambda}_d(1:M)}(g(\text{SNR}, R)) \times f_{\lambda_{1:N+1}}(\lambda_{1:N+1}) \dots f_{\lambda_{N:N+1}}(\lambda_{N:N+1}) d\lambda_{1:N+1} \dots d\lambda_{N:N+1}, \quad (4)$$

As a general case, when $\lambda_{k:N+1} \neq \lambda_{j:N+1}$ for $k \neq j$, $F_{Y|M, \bar{\Lambda}_d(1:M)}(y)$ follows the hypoexponential distribution as

$$F_{Y|M, \bar{\Lambda}_d(1:M)}(y) = 1 - \sum_{k=0}^M A_k \exp(-\lambda_k y), \quad (5)$$

where $A_k = \prod_{j \neq k} \frac{\lambda_j}{\lambda_j - \lambda_k}$ and $\sum_{i=0}^M A_i = 1$ [11]. On the other hand, when $\lambda_{0:N+1} = \lambda_{1:N+1} = \dots = \lambda_{M:N+1} = \lambda$, which corresponds to the co-located antenna array with M elements, $F_{Y|M, \bar{\Lambda}_d(1:M)}(y)$ is the CDF of the gamma distribution as

$$F_{Y|M, \lambda}(y) = 1 - \sum_{k=0}^M \frac{\exp(-\lambda y) \cdot (\lambda y)^k}{k!}. \quad (6)$$

Therefore, as shown in the equation, $F_{Y|M, \bar{\Lambda}_d(1:M)}(y)$ can be simplified into $F_{Y|M, \lambda}(y)$ with the single condition variable λ instead of the condition vector $\bar{\Lambda}_d(1:M)$. Also, the outage probability in (4) can be expressed with a single integral as

$$\tilde{P}_{out} = \sum_{M=0}^N \binom{N}{M} p^{N-M} (1-p)^M \int F_{Y|M, \lambda}(g(\text{SNR}, R)) f_{\lambda|M}(\lambda) d\lambda. \quad (7)$$

We note that, for the co-located approximation, $P_{out} = F_{Y|M=N, \lambda=d_0^\alpha}(g(\text{SNR}, R))$ without any integral, because all the links have the same distances of d_0 to the destination. Compared to (4), the outage equation in (7) is much simpler, because there is only one integral. Also, the conditional CDF $F_{Y|M, \bar{\Lambda}_d(1:M)}(y)$ in (5) is numerically sensitive to compute [1]. Therefore, ultimately to capture the impact of path-loss disparity, we use an approximation to project the vector $\bar{\Lambda}_d(1:M) = [\lambda_{1:N+1}, \dots, \lambda_{M:N+1}]^T$ into a single variable λ assuming high SNR, while keeping the influence of the random relay locations on the outage rate, in the following section.

B. Gamma Approximation of $F_{Y|M, \bar{\Lambda}_d(1:M)}(y)$ into $F_{Y|M, \lambda}(y)$

Many studies on CT focus on the asymptotic performance by the limit of $\text{SNR} \rightarrow \infty$ [1]. In [1], the author proposes a simple but accurate way to calculate outage performance of CT

with dissimilar path losses, where the outage probability based on hypoexponential distribution in (5) can be approximated by the outage probability computation using gamma distribution in (6) with a negligible error. This enables us to use the traditional notion of the performance analysis based on the real multiple-antenna array system to the VMISO link. The key result in this approximation is

$$\lambda = \left(\prod_{k=0}^M \lambda_{k:N+1} \right)^{1/(M+1)}. \quad (8)$$

In other words, in this gamma approximation, the single parameter λ is equal to the geometric average of the distinct $\lambda_{k:N+1}$ for $k = 0, 1, \dots, M$.

C. Approximation of $f_{\lambda|M}(x)$ by the Central Limit Theorem

To calculate the outage rate with the random relay locations in (7) with the gamma approximation, we need to obtain the conditional PDF of λ for given M . In dB, (8) is expressed as

$$10 \log_{10} \lambda = \frac{10}{M+1} \sum_{k=0}^M \log_{10} \lambda_{k:N+1}, \quad (9)$$

where $\lambda_{0:N+1} = d_0^\alpha$ is deterministic, while $\lambda_{1:N+1}, \dots, \lambda_{M:N+1}$ are i.i.d. random variables, when d_0, r_s , and α are given. Therefore, when M is large enough, by the Central Limit Theorem (CLT) [11], $f_{\lambda|M}(x)$ in (7) is approximated into a log-normal distribution as

$$f_{\lambda|M}(x) \approx \frac{1}{x \xi \sqrt{2\pi\sigma}} \exp \left[-\frac{(10 \log_{10} x - \mu)^2}{2\sigma^2} \right], \quad (10)$$

where $0 < x < \infty$, $\xi = \ln 10/10$. Also, because $\lambda_{k:N+1} = 1/d_k^\alpha$, $\mu = \mathbb{E}\{\lambda_{(dB)}|M\} = \frac{10\alpha}{M+1} (\log_{10} d_0 + M \mathbb{E}\{\log_{10} d_k\})$ and $\sigma^2 = \text{VAR}\{\lambda_{(dB)}|M\} = \frac{100\alpha^2 M}{(M+1)^2} \text{VAR}\{\log_{10} d_k\}$.

Therefore, the influence of the random relay locations can be characterized by the log-normal approximation of the PDF of λ , which means that the random separations have the same effect as *log-normal shadowing* on the outage. Using this approximation, the outage probability \tilde{P}_{out} in (7) can be simplified in a summation form using the Gauss-Hermite method [12]:

$$\tilde{P}_{out} \approx \sum_{M=0}^N \binom{N}{M} \frac{p^{N-M} (1-p)^M}{\sqrt{\pi}} \left[\sum_{i=1}^m W_i \cdot G(10^{\frac{\sqrt{2}\sigma r_i + \mu}{10}}) \right]. \quad (11)$$

where $G(x) = F_{Y|M, \lambda=x}(g(\text{SNR}, R))$, W_i are weight factors, r_i are the roots of the Hermite polynomial, and m is the order of the Hermite polynomial. However, the outage probability is determined by the tail property of the channel distribution, and the log-normal approximation has a longer tail than the original conditional PDF $f_{\lambda|M}(x)$, especially when M is small. Therefore, this outage rate based on the log-normal approximation is higher than (7), which is used to derive the upper bound of the outage rate in the following section.

IV. UPPER AND LOWER BOUNDS OF OUTAGE RATE

To calculate the approximated outage probability in the previous section, which serves as an upper bound of the real outage capacity, $\mathbb{E}\{\log_{10} d_k\}$ and $\text{VAR}\{\log_{10} d_k\}$ need to be obtained for μ and σ^2 in (11). However, the PDF of

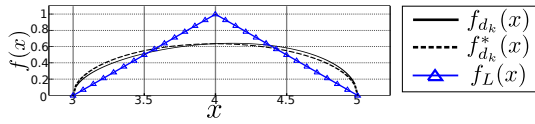


Fig. 3. PDF of d_k and its approximations, when $r_s = 1$ and $d_0 = 4$

d_k , $f_{d_k}(x)$, which characterizes the distance from Relay k to the destination, does not give closed form expressions of its mean and variance¹. Therefore, in this section, we approximate $f_{d_k}(x)$ and derive the corresponding μ and σ^2 in closed forms. Moreover, we also propose upper and lower bounds of the real P_{out} in (2) for $\text{SNR} \rightarrow \infty$.

A. Upper Bound $P_{out:U}$

When d_0 is large enough compared to r_s in Fig. 2, the original PDF of d_k , $f_{d_k}(x)$ can be simplified into $f_{d_k}^*(x) = \frac{2}{\pi r_s^2} \sqrt{r_s^2 - (d_0 - x)^2}$, where $d_0 - r_s \leq x \leq d_0 + r_s$. As an example, in Fig. 3, when $d_0 = 4$ and $r_s = 1$, $f_{d_k}^*(x)$ is indicated by the black dotted line, while the original PDF $f_{d_k}(x)$ is represented by the black solid line. As shown in the figure, $f_{d_k}^*(x) \approx f_{d_k}(x)$ in the domain $d_0 - r_s \leq x \leq d_0 + r_s$, which confirms the validity of $f_{d_k}^*(x)$. Moreover, this approximated PDF $f_{d_k}^*(x)$ has the mean and variance in closed forms as $\mathbb{E}\{d_k\} = d_0$ and $\text{VAR}\{d_k\} = r_s^2/4$. Therefore, by the Taylor expansion, $\mathbb{E}\{\log_{10} d_k\} \approx \log_{10} d_0$ and $\text{VAR}\{\log_{10} d_k\} \approx \frac{r_s^2}{4(d_0 \ln 10)^2}$. Therefore, we can obtain μ and σ^2 as

$$\mu = 10\alpha \log_{10} d_0, \quad (12)$$

$$\sigma^2 = \frac{25M}{(M+1)^2} \left(\frac{\alpha r_s}{d_0 \ln 10} \right)^2. \quad (13)$$

By plugging these two parameters with the worst case first-hop probability $p = p_{max} = 1 - e^{-r_s^\alpha \cdot g(\text{SNR}, R)}$ into (11), the upper bound $P_{out:U}$ of the real P_{out} in (2) can be obtained.

B. Lower Bound $P_{out:L}$

To derive a lower bound of the outage probability, we propose a new PDF $f_L(x)$ that is intentionally designed to obtain a smaller variance σ_L^2 than σ^2 in (13) to shrink the tail probability of the log-normal approximation in (11). The new PDF $f_L(x)$, which is triangle-shaped and symmetric to $x = d_0$ as indicated by the blue line with the triangle markers in Fig. 3, is given by

$$f_L(x) = \begin{cases} \frac{x+r_s-d_0}{r_s^2}, & d_0 - r_s \leq x < d_0, \\ \frac{-x+r_s+d_0}{r_s^2}, & d_0 \leq x < d_0 + r_s, \end{cases} \quad (14)$$

which gives $\mathbb{E}\{L\} = d_0$ that is same to $\mathbb{E}\{d_k\}$ and $\text{VAR}\{L\} = r_s^2/6$ that is smaller than $\text{VAR}\{d_k\}$. Thus, using this PDF $f_L(x)$ and the Taylor expansion, the corresponding μ is same to (12), while the reduced version of σ^2 in (13) is given by $\sigma_L^2 = 2\sigma^2/3$. Therefore, if applying $\sigma^2 = \sigma_L^2$ with the error-free first-hop condition $p = 0$, which always makes $M = N$, in (11), the lower bound of the real outage probability denoted by $P_{out:L}$ can be obtained.

¹We have derived the original PDF of d_k , but space constraints do not allow including it here.

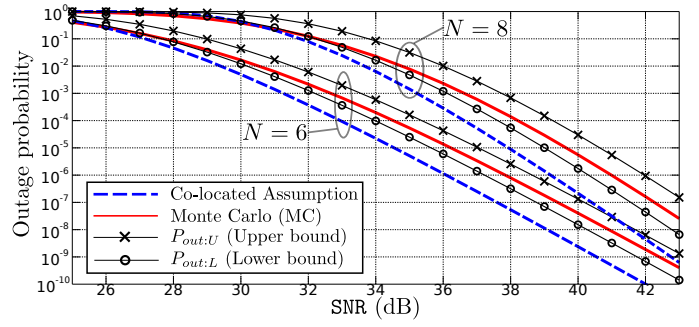


Fig. 4. Outage curves, when $R = 1$, $d_0 = 2$, $r_s = 1$, $\alpha = 4$, and $N = 6, 8$

V. SIMULATION RESULTS AND DISCUSSION

A. Outage Probability

Fig. 4 shows the outage simulation results with $R = 1$, $d_0 = 2$, $r_s = 1$, and $\alpha = 4$. In the figures, the horizontal axis is SNR in dB, while the vertical axis indicates the outage probability. There are two groups of the curves: the group having the higher outage rates with the steeper slopes corresponds to $N = 8$, while the lower group indicates $N = 6$. The blue dashed lines represent the outage rates based on the co-located assumption that ignores the path-loss disparity and first-hop errors. Also, the red solid curves are the true outage probabilities obtained by the Monte Carlo simulation (MC), while the solid lines with the 'x'- and 'o'-markers indicate the upper and lower bounds, respectively. Therefore, the gaps between the blue dashed lines and the red solid lines are the errors caused by the co-located assumption. For example, when the target outage rate is 10^{-6} , the errors are about 1.75 and 1.8dB for $N = 6$ and 8, respectively. In other words, to achieve the outage probability of 10^{-6} considering the relay separations and the source-relay link errors, it requires more transmission power (e.g., 1.75 and 1.8dB for $N = 6$ and 8, respectively) than the transmit power calculated by the co-located approximation.

Moreover, in the both groups, the real outage curves obtained by Monte Carlo simulation are always in between $P_{out:U}$ and $P_{out:L}$ in the high SNR regime (when the outage is less than 10^{-4}), which verifies the two bounds. Therefore, the SNR penalty of the co-located assumption (i.e., the error in terms of SNR to achieve the target outage rate) can be estimated by the two bounds that characterize the impact of the path-loss disparity by the equivalent log-normal shadowing model, following the conventional notion of the composite channel.

B. SNR Penalty depending on System Parameters

In this section, we look at the error of the co-located assumption in terms of the SNR penalty or gap to achieve the outage probability of 10^{-6} depending on three system parameters: the distance ratio d_0/r_s , the path loss exponent α , and the number of relays N . In the simulation results shown in Figs. 5, 6, and 7, there are three SNR gaps to the co-located assumption: the real error based on MC (the red solid lines), and the estimated errors by the upper and lower bounds (the black curves with the 'x'- and 'o'-markers, respectively). In

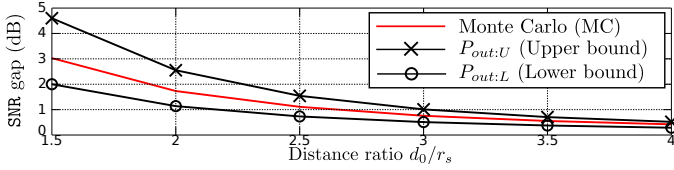


Fig. 5. SNR gaps versus d_0/r_s , when $r_s = 1$, $\alpha = 4$, and $N = 6$

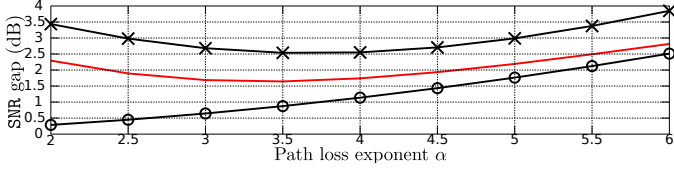


Fig. 6. SNR gaps versus α , when $r_s = 1$, $d_0 = 2$, and $N = 6$

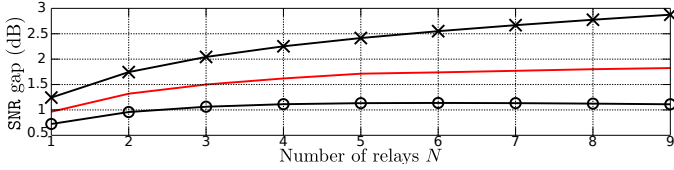


Fig. 7. SNR gaps versus N , when $r_s = 1$, $d_0 = 2$, and $\alpha = 4$

the three figures, the real error is always in between the errors measured by the two bounds.

Fig. 5 shows the SNR penalty in dB indicated by the y-axis for the different distance ratio d_0/r_s represented by the x-axis, when $r_s = 1$, $\alpha = 4$ and $N = 6$. All the three SNR gaps decrease as d_0/r_s increases, because the impact of the path-loss disparity becomes negligible for high d_0/r_s , which is also noticed by that the two variances σ^2 and σ_l^2 of the equivalent log-normal shadowing model are decreasing functions of d_0/r_s . Also, the first-hop error ignored in the co-located assumption is relatively much smaller than the second-hop error, when d_0/r_s is large. However, considering that $d_0/r_s=1.5$ and 2 are the CT range extension ratios widely assumed in the VMISO-based protocol studies, the corresponding errors are large enough to degrade the protocols designed and operated with the co-located assumption.

Fig. 6 displays the impact of the path loss exponent α on the SNR penalty, when $r_s = 1$, $d_0 = 2$, and $N = 6$. The SNR gaps based on the MC and the upper bound have the convex curves that have the minimum heights at around $\alpha = 3.5$, while the lower bound is monotonically increasing. The height decreases of the MC and the upper bounds for $2 \leq \alpha \leq 3.5$ are because the first-hop error relative to the second-hop error increases as α decreases for a fixed d_0/r_s , which means that the first-hop error cannot be ignored in this range. The reason that the lower bound simply increases in this range is also the error-free first-hop assumption. On the other hand, when $3.5 \leq \alpha \leq 6$, all the three curves increase, as α increases, because the path-loss disparity within the VMISO cluster becomes significant (σ^2 and σ_l^2 are increasing functions of α).

In the last figure, Fig 7, the three graphs increase, while the slopes become less steep, as N increases. This pattern can be explained by the equivalent shadowing model: the path-loss disparity can be characterized the same (fully-correlated) shadowing outcomes overlaid on the independent Rayleigh

fading channels of N antennas in the real MISO link. Thus, by the path-loss disparity, the VMISO link loses a certain degree of the diversity gain because of the increased channel correlation compared to the full diversity in the co-located assumption simply over independent Rayleigh fading. Therefore, the SNR penalty to the co-located assumption increases, as N increases, if the degree (variance) of the equivalent shadowing is fixed. However, the variances used in the two bounds (σ^2 and σ_l^2) decrease, when $N=M$ (assuming the error-free first-hop) increases. Thus, the slopes of the graphs become less steep, as N increases. Moreover, the MC and the upper bound always have higher slope than the lower bound, because of the diversity gain losses in the MC and the upper bounds are more significant by the first-hop error.

VI. CONCLUSION

In this paper, we analyze the impact of the path-loss disparity in the VMISO link, where physically-separated multiple nodes transmit together to a single destination node, using the high SNR assumption. By the asymptotic analysis ($\text{SNR} \rightarrow \infty$) of the outage capacity, we show that the performance loss by the path-loss disparity has the same model as log-normal shadowing. The simulation results show how the error of the co-located assumption changes depending on the system parameters such as d_0/r_s , α , and N . Moreover, the derived bounds can be used to estimate this error of the co-located VMISO model in the high SNR regime.

REFERENCES

- [1] J. Laneman, "Limiting analysis of outage probabilities for diversity schemes in fading channels," in *Proc. IEEE GLOBECOM*, vol. 3, pp. 1242 – 1246 vol.3, Dec. 2003.
- [2] N. C. Beaulieu and J. Hu, "A closed-form expression for the outage probability of decode-and-forward relaying in dissimilar rayleigh fading channels," *IEEE Commun. Letters*, vol. 10, no. 12, pp. 813 –815, december 2006.
- [3] G. Jakkari, S. V. Krishnamurthy, M. Faloutsos, P. V. Krishnamurthy, and O. Ercetin, "A cross-layer framework for exploiting virtual MISO links in mobile ad hoc networks," *IEEE Trans. Mobile Computing*, vol. 6, no. 6, pp. 579 –594, June 2007.
- [4] S. Lakshmanan and R. Sivakumar, "Diversity routing for multi-hop wireless networks with cooperative transmissions," in *Proc. IEEE SECON*, pp. 1 –9, June 2009.
- [5] J. W. Jung and M. A. Ingram, "Residual-energy activated cooperative transmission (REACT) to avoid the energy hole," in *Proc. IEEE ICC*, June 2010.
- [6] L. Thanayankizil, A. Kailas, and M. A. Ingram, "Routing for wireless sensor networks with an opportunistic large array (OLA) physical layer," *Ad Hoc & Sensor Wireless Networks*, vol. 8, no. 1-2, pp. 79–117, 2009.
- [7] B. Sirkeci-Mergen, A. Scaglione, and G. Mergen, "Asymptotic analysis of multistage cooperative broadcast in wireless networks," *IEEE Trans. Inf. Theory*, vol. 52, no. 6, pp. 2531–2550, June 2006.
- [8] B. Bash, D. Goeckel, and D. Towsley, "Clustering in cooperative networks," in *Proc. IEEE INFOCOM 2011*, pp. 486 –490, Apr. 2011.
- [9] A. Scaglione, D. Goeckel, and J. Laneman, "Cooperative communications in mobile ad hoc networks," *IEEE Sig. Proc. Magazine*, vol. 23, no. 5, pp. 18 – 29, Sept. 2006.
- [10] H. Jung, Y. Chang, and M. A. Ingram, "Experimental range extension of concurrent cooperative transmission in indoor environments at 2.4GHz," in *Proc. IEEE MILCOM*, Oct. 2010.
- [11] S. Ross, *Introduction to Probability Models*, 2000.
- [12] M. Abramowitz and I. A. Stegun, *Handbook of Mathematical Functions 10th Printing with Corrections*. Dover, New York, 1972.